

Horita, J., and M. E. Berndt (1999), Abiogenic methane formation and isotopic fractionation under hydrothermal conditions, *Science*, 285, 1055–1057.

House, C. H., et al. (2003), Carbon isotopic fractionation by Archeans and other thermophilic prokaryotes, *Org. Geochem.*, 34, 345–356.

Kelley, D. S., et al. (2005), A serpentinite-hosted ecosystem: The lost city hydrothermal field, *Science*, 307, 1428–1434.

Krasnopolsky, V. A., et al. (2004), Detection of methane in the Martian atmosphere: Evidence for life?, *Icarus*, 172, 537–547.

Lyons, J. R., et al. (2005), Formation of methane on Mars by fluid-rock interaction in the crust, *Geophys. Res. Lett.*, 32, L13201, doi:10.1029/2004GL022161.

McCullom, T. M. (2003), Formation of meteorite hydrocarbons from thermal decomposition of siderite (FeCO<sub>3</sub>), *Geochim. Cosmochim. Acta*, 67, 311–317.

Mumma, M. J., et al. (2004), Detection and mapping of methane and water on Mars, *Bull. Am. Astron. Soc.*, 36, 1127.

Nair, H., et al. (2005), Isotopic fractionation of methane in the Martian atmosphere, *Icarus*, 175, 32–35.

Oehler, D. Z., et al. (2005), Impact metamorphism of subsurface organic matter on Mars: A potential source for methane and surface alteration, paper presented at the 36th Lunar and Planetary Science Conference, Lunar and Planet. Inst., Houston, Tex., 14–18 March.

Onstott, T. C., et al. (2006), Martian CH<sub>4</sub> sources, flux, and detection, *Astrobiology*, 6, 377–395.

Oze, C., and M. Sharma (2005), Have olivine, will gas: Serpentinization and the abiogenic production of methane on Mars, *Geophys. Res. Lett.*, 32, L10203, doi:10.1029/2005GL022691.

Sherwood Lollar, B., et al. (2002), Abiogenic formation of alkanes in the Earth's crust as a minor source for global hydrocarbon reservoirs, *Nature*, 416, 522–524.

Welhan, J. A., and H. Craig (1983), Methane and helium in deep Earth gases, *Abstr. Pap. Am. Chem. Soc.*, 186, 14-GEOC.

Allen@jpl.nasa.gov; Barbara Sherwood Lollar, Department of Geology, University of Toronto, Canada; Bruce Runnegar, NASA Astrobiology Institute, NASA Ames Research Center, Moffett Field, Calif.; Dorothy Z. Oehler, NASA Johnson Space Center, Houston, Tex.; James R. Lyons, Institute of Geophysics and Planetary Physics, University of California, Los Angeles (UCLA); Craig E. Manning, Department of Earth and Space Sciences, UCLA; and Michael E. Summers, Department of Physics and Astronomy, George Mason University, Fairfax, Va.

#### Author Information

Mark Allen, Jet Propulsion Laboratory, California Institute of Technology, Pasadena; E-mail: Mark.

## A View of Hurricane Katrina With Early 21st Century Technology

PAGES 433, 440

Observing, modeling, and forecasting systems have been undergoing rapid development in the past two to three decades. For example, Atlantic hurricanes are closely monitored by the U.S. National Oceanic and Atmospheric Administration's (NOAA) National Weather Service through a significantly improved upper-air and ground-based observational network supplemented by aircraft, ship, and ocean buoy data. Given initial conditions and lateral boundary conditions provided by larger-scale model analyses, regional models have been widely utilized to predict hurricane track and intensity.

Nowadays, satellite observations are playing an increasingly important role in providing global estimations of precipitation, radiative fluxes, clouds, and winds, with unprecedented temporal and spatial coverage. Global atmospheric models and global operational analyses are moving toward providing forecasts and products at resolutions ranging from 0.1° to 0.5° (10–50 kilometers). There is evidence that improved hurricane structure and track forecasts could result in part from such increases in model resolution.

These advances in global modeling eventually could eliminate the need for regional hurricane forecast models and the associated concerns with the need to specify lateral boundary conditions. Yet these advances also present interesting challenges to the atmospheric modeling and parameterization communities because, at these resolutions, some assumptions made in model sub-grid-scale

parameterizations are marginally valid. Evaluating these new developments in global models and observing systems, particularly their representation of physical and dynamical processes affecting hurricanes, is a necessary and important step toward improving hurricane forecasting.

Hurricane Katrina in 2005 was one of the most devastating tropical cyclones ever to hit the United States. The official death toll is more than 1300, and the estimated damage is more than US\$200 billion. Even though it weakened from Category 5 to Category 3 before making landfall [Knabb *et al.*, 2005],

Hurricane Katrina produced massive damage in Louisiana, Mississippi, and Alabama, and severely affected millions of people. In the interest of highlighting present-day observation and global model forecasting capabilities, this article presents high-resolution satellite observations of rainfall, clouds, wind, and sea surface temperatures (SST) to document the evolution of Hurricane Katrina. The analysis uses the European Centre for Medium-Range Weather Forecasts (ECMWF) global forecasts and the NASA Goddard Earth Observing System Version 5 (GEOS-5) global forecasts alongside satellite observations, with a focus on precipitation and cloud processes.

#### Observations and Global Model Forecasts

Rainfall retrievals from a five-satellite constellation—including the Tropical Rainfall

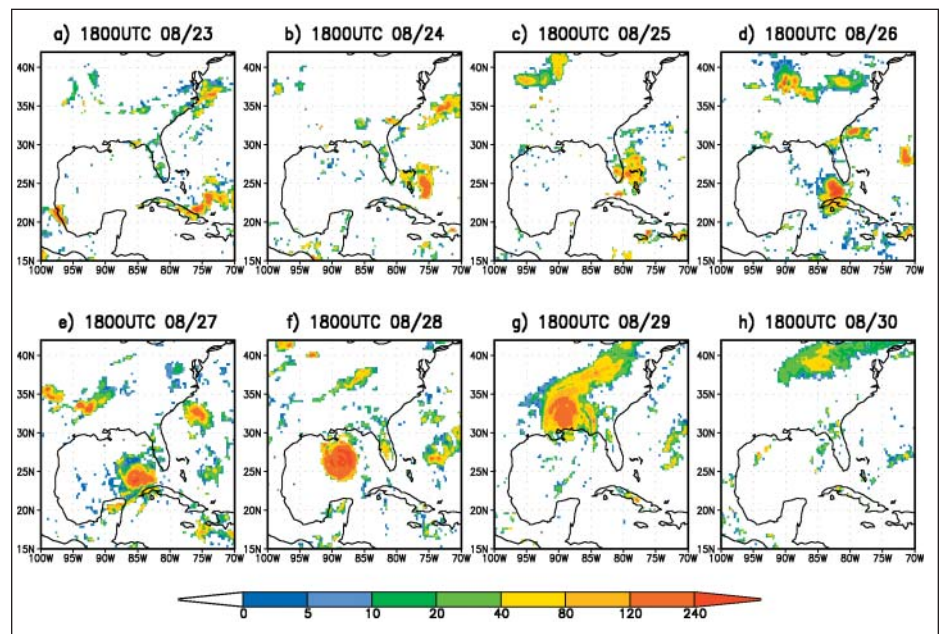


Fig. 1. Horizontal distributions of six-hour averaged microwave rainfall retrievals (millimeters per day, 0.25 × 0.25 degrees) centered at 1800 UTC from 23 to 30 August 2005.

By X. LIN, J.-L. F. LI, M. J. SUAREZ, A. M. TOMPKINS, D. E. WALISER, M. M. RIENECKER, J. BACMEISTER, J. H. JIANG, C. M. TASSONE, J.-D. CHERN, B. CHEN, AND H. SU

Measuring Mission (TRMM); the Defense Meteorological Satellite Program (DMSP) F13, F14, and F15 satellites; and the Earth Observing System (EOS) Aqua satellite—were merged in this study to provide global, six-hour coverage of Hurricane Katrina. They are supplemented by Advanced Microwave Sounding Unit-B (AMSU-B) rainfall retrievals from the NOAA-15, -16, and -17 satellites.

Cloud-top and cloud optical properties were computed from pixel data collected by the Moderate Resolution Imaging Spectroradiometer (MODIS) on the EOS satellites Terra and Aqua. Daily TRMM Microwave Imager (TMI) derived SSTs, and QuikSCAT Level 3 ocean wind vectors were also used in the analyses.

The five-day operational forecasts at T799 spectral resolution (approximately 25 kilometer equivalent grid spacing) from the ECMWF Integrated Forecasting System (IFS) were used. The forecasts were initialized with the ECMWF four-dimensional variational analyses. The NASA GEOS-5 model's prognostics and diagnostics were computed at  $0.25^\circ \times 0.33^\circ$  resolution in the horizontal. The forecast presented here is from a five-day experimental run initialized with NOAA's National Centers for Environmental Prediction (NCEP) T382 analysis.

#### Satellite View of Katrina

Figure 1 shows six-hour averaged rain rates centered at 1800 UTC from 23 to 30 August 2005. Katrina originated as a tropical depression over the southeastern Bahamas on 23 August 2005 (Figure 1a). It strengthened into Tropical Storm Katrina the next day and gradually moved westward, making landfall on the southeastern coast of Florida at about 2300 UTC on 25 August. During this period, the Gulf of Mexico was dominated by clear-sky conditions with scattered, isolated clouds (not shown). SSTs averaged over the central Gulf region were warm, generally above  $30^\circ\text{C}$  on August 25 and slowly increasing up to  $30.6^\circ\text{C}$  on August 27 (Figure 2a). These variations provided favorable conditions for enhanced deep convection and a strengthening of the hurricane.

After passing southern Florida as a weak Category 1 hurricane (Figures 1b and 1c), Katrina intensified rapidly over the warm waters of the Gulf of Mexico between 26 and 28 August (Figures 1d, 1e, and 1f), with estimated highest sustained winds of 175 miles per hour (78 meters per second) [Knabb *et al.*, 2005]. Convection and clouds became more organized in a spiral pattern, and precipitation was more widespread and intensive, with the heaviest rain rate exceeding 10 millimeters per hour near the eye wall. Merged microwave rain retrievals, MODIS cloud-top temperature, and cloud optical thickness, averaged between  $24\text{--}29^\circ\text{N}$  and  $92\text{--}85^\circ\text{W}$ , correspond nicely with one another (Figures 2a and 2b). Although the wind retrievals are underestimates due to rain effects and resolution, QuikSCAT data indicated ocean surface wind speed

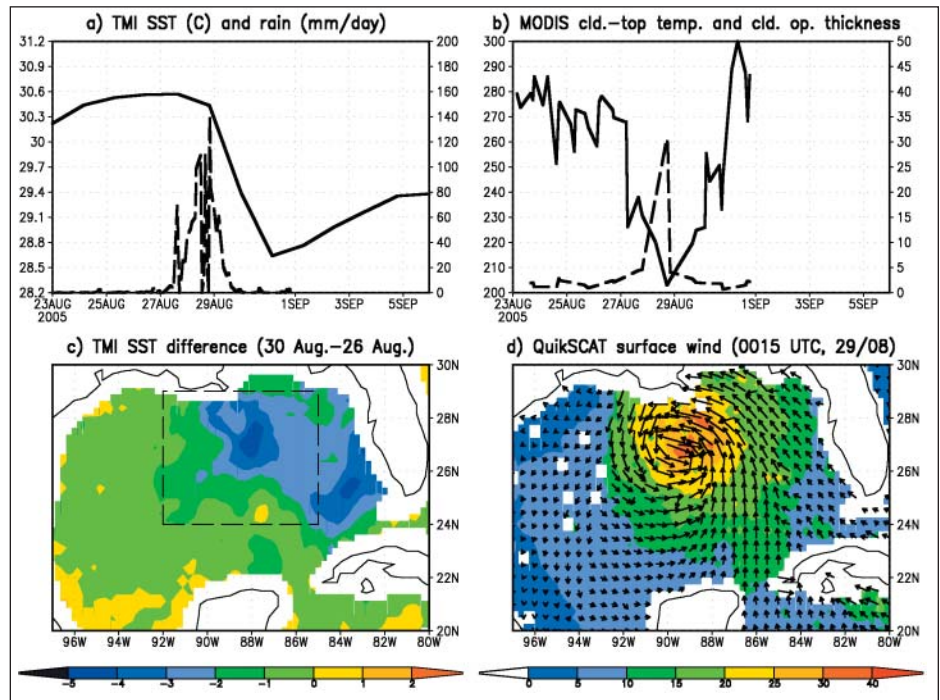


Fig. 2. (a) Time series of TMI-derived daily SST ( $^\circ\text{C}$ , solid curve) and hourly microwave rain retrievals (millimeters per day, dashed curve) averaged between  $24\text{--}29^\circ\text{N}$  and  $92\text{--}85^\circ\text{W}$  (the dashed box shown in Figure 2c). (b) Time series of MODIS cloud-top temperature (K, solid curve) and cloud optical thickness (dashed curve) averaged between  $24\text{--}29^\circ\text{N}$  and  $92\text{--}85^\circ\text{W}$ . (c) SST difference (K) between conditions before and after the passage of Hurricane Katrina. (d) QuikSCAT ocean surface wind speed (meters per second) and wind vectors (descending node) at 0015 UTC, 29 August 2005.

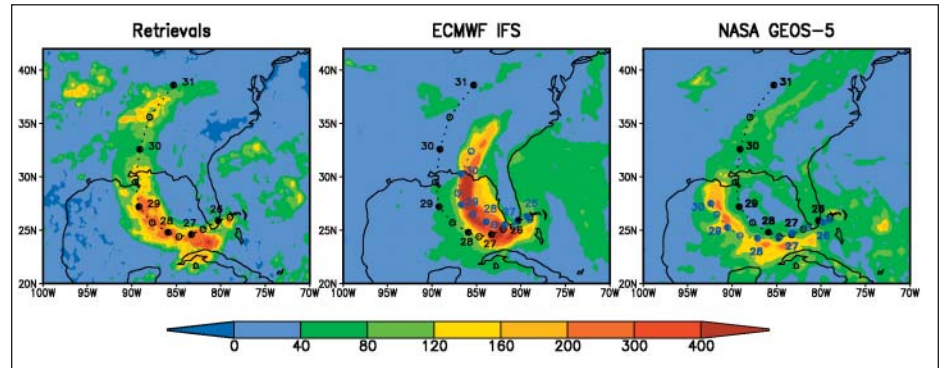


Fig. 3. Accumulated five-day surface rainfall (millimeters) from satellite retrievals, and from single forecasts by the ECMWF IFS and the NASA GEOS-5 high-resolution global models. The official NHC observed 'best track' (black curve) and the forecast tracks (blue curve) for Katrina are superimposed. The solid circles represent positions at 0000 UT, while the open circles represent positions at 1200 UT. The ECMWF and NASA forecasts are initialized at 1200 and 0600 UT, respectively, 25 August 2005.

above 30 meters per second around the hurricane center (Figure 2d).

SSTs averaged along the hurricane track started to decrease after the passage of Katrina, and the lowest SST ( $28.6^\circ\text{C}$ ) occurred about three to four days later when Katrina had already made landfall, suggesting a strong entrainment of deeper, cooler ocean water resulting from strong mixing induced by the hurricane [Price, 1981].

Katrina made landfall near the Louisiana-Mississippi border around 1500 UTC on 29 August, and it started to weaken as it moved northward and inland (Figure 1g).

However, the hurricane still was a large system, and precipitation was heavy and widespread. The heaviest rain rate was more than five millimeters per hour around the center. By 1800 UTC on 30 August (Figure 1h), Katrina had weakened into a tropical depression. During this time, local SSTs along the hurricane track over the Gulf of Mexico decreased by  $3\text{--}5^\circ\text{C}$  compared with the prehurricane SSTs (Figure 2c) before slowly recovering on 31 August. After 30 August, the Katrina-related rainband moved to midlatitudes and merged with an extratropical wave to become a mid-latitude frontal rainband.



### Comparison of Early Model Forecasts With Satellite Data

The evaluation of hurricane forecast skill requires ensembles of historical forecasts. The purpose of this article is not to undertake such an evaluation, but rather to demonstrate the current status of satellite physical retrievals and their potential to provide valuable information for such evaluations and contribute to model improvements. Figure 3 shows a pictorial example of the 120-hour accumulated surface rainfall from satellite retrievals, and from single high-resolution forecasts from ECMWF and NASA models.

Predictions of Hurricane Katrina were statistically better than the historical forecast skill [e.g., *Knabb et al.*, 2005]. Similarly, ECMWF as well as NASA high-resolution global forecasts performed remarkably well during the first two days, with the forecast tracks closely matching what was observed for Katrina, and only small displacement errors. In the model, the heaviest rainfall during the first 48 hours was not near the storm center, but rather was about 80–120 kilometers to the south of the hurricane track, similar to what was observed. This interesting feature cannot be identified by examining the dynamical fields alone. Overall, the amplitude of the model accumulated rain amount is similar to satellite microwave retrievals, although the GEOS model shows a slightly lower amount while the ECMWF model shows a slightly higher amount. Track displacements start to amplify in the 96–120 hour forecasts, but the errors are still in line with the mean errors of the NOAA National Hurricane Center (NHC) official forecasts.

The simulated Katrina in the NASA model tends to move more slowly and remains over the Gulf of Mexico. The forecasted track deviates by two to three degrees west of the best track.

The hurricane in the ECMWF forecast, though, deviates by two to three degrees east of the best track, and makes landfall between Alabama and Florida about 12 hours late. These differences in the hurricane track and accumulated precipitation may reflect inadequacies in the large-scale circulation provided in the initial conditions, or imperfect model physical parameterizations, but also may be due to the system's lack of predictability.

### Developments in Hurricane Forecasts

Advances in spaceborne observations and numerical weather prediction (NWP) models provide new opportunities for improving hurricane forecasts. Apart from their importance for NWP, global atmospheric models of hurricanes and their forecasts represent an important and unique test bed of model formulations.

Recent developments that include moving from synoptic-scale-resolving to mesoscale-resolving global models show some very encouraging results. In addition to increasing resolution and including more physically based parameterizations on mesoscale effects in conventional general circulation models, cloud-scale-resolving global models—in which the cloud dynamics and mesoscale processes are explicitly resolved—also are being developed and could be used as a parallel approach to more realistically simulate hurricanes in global models in the future.

Better resolution of the hurricane structure and larger-scale steering circulation, along with improved initial conditions provided by high-resolution satellite data and sophisticated data assimilation systems, could lead to better detection, monitoring, understanding, and prediction of the genesis and development of hurricanes that have such a devastating impact on society.

### Acknowledgments

The TRMM TMI, SSM/I, and MODIS data were provided by the NASA Goddard Space Flight Center Data Archive and Distribution Center. The AQUA AMSR-E data were provided by the National Snow and Ice Data Center Distributed Active Archive Center. The QuikSCAT data were obtained from the Physical Oceanography Distributed Active Archive Center at the NASA Jet Propulsion Laboratory. Constructive comments from Naomi Surgi (NOAA/NCEP) and two anonymous reviewers are gratefully acknowledged.

### References

- Knabb R. D., J. R. Rhome, and D. P. Brown (2005), Tropical cyclone report: Hurricane Katrina, 2005, Natl. Hurricane Cent. (Available at [http://www.nhc.noaa.gov/pdf/TCR-AL122005\\_Katrina.pdf](http://www.nhc.noaa.gov/pdf/TCR-AL122005_Katrina.pdf))  
Price, J. F. (1981): Upper ocean response to a hurricane, *J. Phys. Oceanogr.*, 11, 153–175.

### Author Information

Xin Lin, NASA Goddard Space Flight Center (GSFC), Greenbelt, Md., and University of Maryland, Baltimore County (UMBC), Baltimore, E-mail: [mlin@gmao.gsfc.nasa.gov](mailto:mlin@gmao.gsfc.nasa.gov); Jui-Lin F. Li, Jet Propulsion Laboratory (JPL), California Institute of Technology (Caltech), Pasadena, and SkillStorm, Inc., Pasadena, Calif.; Max J. Suarez, NASA GSFC; Adrian M. Tompkins, European Centre for Medium-Range Weather Forecasts, Reading, U.K.; Duane E. Waliser, JPL, Caltech; Michele M. Rienecker, NASA GSFC; Julio Bacmeister, NASA GSFC and UMBC; Jonathan H. Jiang, JPL, Caltech; Huey-Tzu Wu, NASA GSFC and Science and Systems and Application, Inc., Lanham, Md.; Caterina M. Tassone, NASA GSFC and Science Applications International Corporation (SAIC), Beltsville, Md.; Jiun-Dar Chern, NASA GSFC and UMBC; Baode Chen, NASA GSFC and SAIC; and Hui Su, JPL, Caltech.

## Ice-Tethered Profilers Sample the Upper Arctic Ocean

PAGES 434, 438

Studies conducted over the past decade indicate that the Arctic may be both a sensitive indicator of climate change and an active agent in climate variability. Although progress has been made in understanding the Arctic's coupled atmosphere-ice-ocean system, documentation of its evolution is hindered by a sparse data archive. This observational gap represents a critical shortcoming of the 'global' ocean observing system's ability to quantify the complex interrelated atmospheric, oceanic, and terrestrial changes now under way

throughout the Arctic and that have demonstrated repercussions for society [*Symon et al.*, 2005].

Motivated by the Argo float program, an international effort to maintain an ensemble of approximately 3000 autonomous profiling instruments throughout the temperate oceans (see <http://w3.jcommops.org>), a new instrument, the 'Ice-Tethered Profiler' (ITP) was conceived to repeatedly sample the properties of the ice-covered Arctic Ocean at high vertical resolution over time periods of up to three years.

Several prototype ITPs have now been deployed within the Beaufort Gyre system of the Canada Basin. The two systems installed in August 2005 returned temperature and salinity profiles every six hours between a 10- and 760-meter depth for more than a year,

revealing interesting spatial and temporal variations in the regional water masses.

On the basis of these results, five new ITP systems were constructed. Three of these were deployed in the Canada Basin in August/September 2006; the two remaining will be installed in spring 2007 about the North Pole. Plans are being developed internationally to deploy a basin-scale array of profiling instruments during the upcoming International Polar Year (March 2007 to March 2009).

### Technology

The ITP represents the marriage of two related technologies: the profiling Argo float [*Gould et al.*, 2004] and the moored profiler [*Doherty et al.*, 1999]. The ITP system consists of three components: a surface instrument package that sits atop an ice floe; a weighted, plastic-jacketed wire rope tether of arbitrary length (up to 800 meters) suspended from the surface package; and an instrumented underwater unit that travels up and down the wire tether [*Krishfield et al.*, 2006].

By J. TOOLE, R. KRISHFIELD, A. PROSHUTINSKY, C. ASHJIAN, K. DOHERTY, D. FRYE, T. HAMMAR, J. KEMP, D. PETERS, M.-L. TIMMERMANS, K. VON DER HEYDT, G. PACKARD, AND T. SHANAHAN